Volume 1, Number 1 (September 2005) p. 87-102
Revista IBRACON de Estruturas
IBRACON Structural Journal

Plastic strain quantification in reinforced concrete columns

Quantificação das deformações plásticas em pilares de concreto armado

R. A. K. SANCHES [a]
S. RODRIGUES [a]
G. FABRO [b]
F. L. WILLRICH [c]
H. C. LIMA JÚNIOR [d]
correialima@unioeste.br

Abstract

This paper presents a study of the effect of strain gage length on the curve load vs. axial strain of the reinforced concrete columns. Columns 50, 75 and 100 cm high were tested, which were cast with the same concrete compressive strength, ratio of longitudinal and transversal reinforcement. Curves load vs. strain are presented, from which the ductility indexes were calculated and analyzed through variance analysis. The ascendant, as also the descendant branch of the load vs. strain curve is affected by the strain gage length. The formation of the shear plane starts at the beginning of the plasticity process; then, from this point on, it is observed that all the plastic displacements are localized at this plane. This process interferes directly at the usual calculus methodology of strains. Finally, a new methodology to calculate inelastic strains is proposed, which is unaffected by the strain gage length.

Keywords: columns; ductility; strain gage length; scale.

Resumo

Este artigo apresenta um estudo sobre os efeitos do comprimento de avaliação das deformações no diagrama força vs. deformação de pilares de concreto armado. Para tanto foram ensaiados pilares com alturas de 50, 75 e 100 cm, os quais apresentavam mesma resistência à compressão do concreto, taxas de armadura transversais e longitudinais. Apresentam-se curvas força vs. deformação, das quais foram calculados os índices de ductilidade de cada pilar e, em seguida, avaliados por meio de analise de variância. Observou-se que o tanto o comportamento ascendente quanto descendente da curva força vs. deformação axial são influenciados pelo comprimento de avaliação das deformações. A formação do plano de cisalhamento inicia-se no início do processo de plastificação do concreto, então, a partir deste ponto, observa-se que todos os deslocamentos plásticos são localizados neste plano. Este processo interfere diretamente na metodologia usual de cálculo das deformações. Finalmente, é proposta uma nova metodologia simplificada para o cálculo das deformações plásticas em pilares que não é influenciada pelo comprimento de avaliação das deformações.

Palavras-chave: pilares; ductilidade; comprimento de avaliação das deformações; escala.

[a] Civil engineer, State University of Parana West/UNIOESTE
[b] Member and local director of IBRACON, Laboratório de Tecnologia do Concreto da Hidrelétrica de Itaipu/Binacional
[c] Member and local director of IBRACON, Assistant Professor at State University of Parana West /UNIOESTE
[d] Member and local director of IBRACON, Adjunct Professor at State University of Parana West /UNIOESTE. Centro de Ciências Exatas e Tecnológicas, Laboratório de Modelos Reduzidos, Phone: 55 45 220-3221, R. Universitária 2069, Jardim Universitário, CEP.: 85814-110 – Cascavel – PR – Brasil

1 Introduction

With the wide spread of the high-strength concrete, the discussion about ductility of reinforced concrete structures has increased [1]. This fact is base on the lacking of plastic deformation, when the high-strength concrete is overloaded to failure under compression. In addition, the main application of this material is in structures that basically work under compression, such as columns.

The concrete ductility is usually evaluated by its stress vs. strain diagram, which is carried out by compressive test of cylindrical specimens and depends on the intrinsic material properties and the test set up. In the other hand, the concrete column ductility is evaluated by the load vs. strain diagram. In this case, not only does the ductility depend on the intrinsic properties of the materials that comprised the column, but also some others factors, such as: geometry of the structural element, boundary conditions, load type and the constitutive material interaction [2]. When a concrete column is tested under load control, a load vs. strain diagram composed by an ascendant and a descendant branch is gotten. When high-strength concrete columns are analyzed, the strain gradient over the columns is almost null, up to 95% of the peak load [3]. Whereas, the strain uniformity is only observed up to 60% of the peak load, when normal-strength concrete columns are tested [4]. To high load values, a small plastification region is observed, whose localization happens in a random mode over the column height. This region is usually formed in a cross section that presents the highest number of concrete defects and/or the geometry imperfections of the longitudinal bars.

After the peak load, the column load capacity is reduced, which is characterized by the descendant branch of the load vs. strain diagram. At this moment, the plastified region is transformed in a failure region, characterized by a well defined shear plane that is showed in Figure 1. According to Câmara et al. [5], this plane is always perpendicular to the small dimension of column cross section and is a function of the concrete strength and the transversal reinforcement ratio. With the shear plane formation, a reduction on the strains in all column cross section, which are not sectionalized by this plane, is observed. In addition, it is verified that all shortening displacements occur in the region sectionalized by the shear plane.

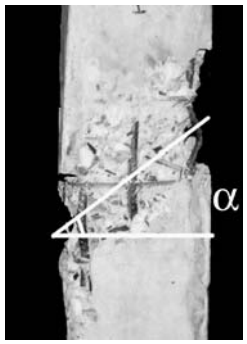

Figure 1 - Rupture shear plane.

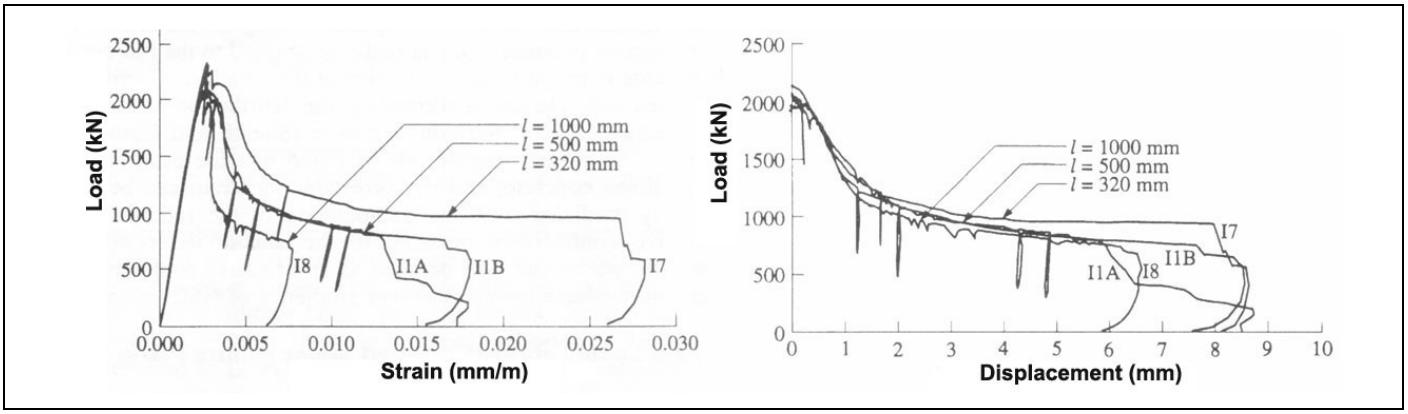

Figure 2 - Load vs. specific strain and load vs. displacement diagrams to columns with different height. (Adapted from Cusson et al., 1996).

Using stereophotogrametry, Torrenti et al. [6] showed that the shear plane formation happens when the peak load is reached. Based on this fact, it is verified that the shortening displacements measured after the peak load in columns with different heights, but with the same physical characteristics, are almost the same [7], implying that columns with higher heights present lower ductility index, when the load vs. strain diagrams are analyzed and confronted. This behavior is exemplified in Figure 2.

This paper aimed to study the variations on the column load vs. strain diagrams, carried out with different strain gage lengths, and to propose a adequate and simplified procedure to calculate the column plastic strain.

2 Ductility evaluation of reinforced concrete columns

Van Vlack [8] defines ductility as the strain measure that indicates the capacity of a body to deform inelastically without losing the strength capacity abruptly. There is a huge controversy about the ideal methodology to quantify the reinforcement concrete column ductility. Some researches conduct their analysis considering only a qualitative evaluation of the load vs. strain diagrams; while, others use only the descendant branch of the load vs. strain diagram to quantify the column ductility [9-10]. Although the later procedure be criticized because it despised all the inelastic strain of the ascendant branch that in the case of

normal-strength concrete column is highly significant, it is widely accepted. Additionally, another point of divergence is the choice of the point used to quantify the plastic strain in the descendant branch. Some researches consider 85% of the peak load as the ideal point [10], other 50% [11]. Nevertheless, if those points are considered contradictories ductility index can be found out, when the parametric load vs. strain diagram is used [12].

To analyze the ductility behavior of the reinforced concrete columns, the ductility index proposed by [13] was used, which is based on the analysis of all points of the descendent branch of the load vs. strain curve, and because of this, it shows higher consistence. Thus, initially, a parametric strain is calculated, on basis of Eq.(1):

$$D_{Pós} = \frac{\int_{\varepsilon p}^{n\cdot\varepsilon p} F_u(\varepsilon)d\varepsilon}{F_u} \quad (1)$$

where, ε_p is the specific strain correspondent to the peak load, and F_u (ε) is the function that governs the load vs. strain behavior of column and n is a coefficient that set bounds to the region analysis, that according to Lima Jr. and Giongo [13] must be taken equal to 3. The post peak ductility index is defined as the ratio between the parametric strain calculated on the basis of Eq.(1) and the peak strain, and can be calculated by Eq. (2):

$$ID_{Pós} = \frac{D_{Pós}}{\varepsilon_p} \quad (2)$$

3 Materials and experimental program

3.1 Materials

Local river sand with fineness modulus of 2.11, maximum size of 2.4 mm and specific mass of 1.64 kg/dm³ was used [14-15]. The crushed aggregated was basaltic with fineness modulus, maximum size and specific mass of 6.8, 19 mm and 1.42 kg/dm³, respectively [14, 16]. Type V Portland cement was used. The mortar rate and the water/dried material ratio were 51% and 10, respectively, for all mixtures and the slump 80±10 mm. The mix design was 1:1.99:2.87 (cement:sand:aggregate) with water/cement ratio of 0.53 and average compressive strength of 34.4 MPa.

The longitudinal bars were 8 mm diameter; with steel yield strength of 660 MPa and elasticity modulus of 215 GPa. The transversal reinforcement was comprised by 4.2 mm diameter ties, with yield strength and elastic modulus of 675 MPa and 198 GPa, respectively.

3.2 Specimens details

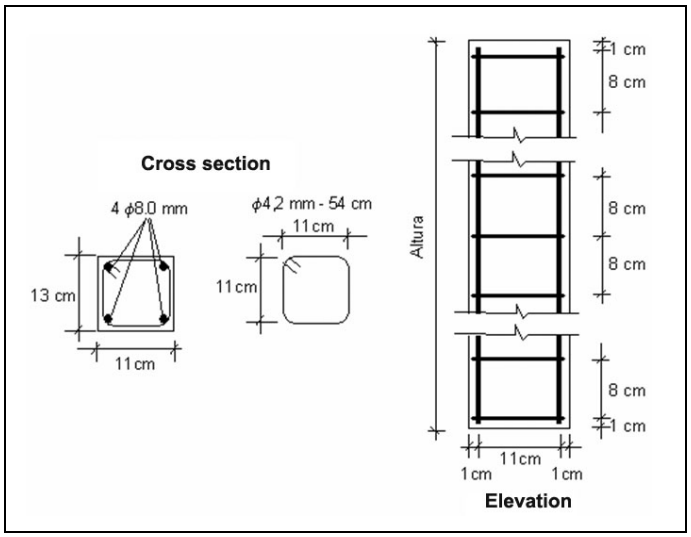

Figure 3 - Column geometry.

The columns were 50, 75 and 100 cm high and had 15 cm square cross section, being cast two columns for each height. The longitudinal reinforcement was the same for all columns and was comprised by four bars of 8 mm diameter. The transversal reinforcement were comprised by 4.2 mm diameter ties with 135° hooks extending 10 times the bar diameter and tie spacing of 8 cm, which was calculated based on the Brazilian Code [17].

The columns were cast vertically using steel formwork and internal vibration, using only one concrete batch. This procedure aimed to keep uniformity on the concrete elastic properties of all columns. Six 15x30 cm cylinders were also cast to compressive test. After being cast, the columns tops were covered with plastic sheets, which were kept in place for 24 hours. Then they were stripped, watering and completely covered with plastic sheet until the geometry of a typical column specimen is illustrated.

Table 1 - Columns characteristics.

Column	*h* (cm)	f_{cj} (MPa)	f_{ck} (MPa)	ρ_l (%)	ρ_t (%)	F_u (kN)	ε_p (‰)	σ_c (MPa)	σ_s (MPa)	α	$ID_{pós}$
P 50-1	50	34,14	34,38	1,2	0,451	710,2	4,032	34,58	660	46,7°	1,485
P 50-2						721,0	4,068	35,23	660	44,0°	1,559
P 75-1	75					657,2	3,145	31,41	660	47,5°	1,398
P 75-2						740,6	3,124	36,40	660	42,0°	1,288
P 100-1	100					701,4	2,653	35,13	570	45,0°	1,148
P 100-2						686,7	2,706	34,11	582	49,0°	1,194

Note.: h is the column height, f_{ck} is the characteristic concrete compressive strength, f_{cj} is the mean concrete compressive strength, ρ_l is the longitudinal reinforcement ratio, ρ_t is the transversal reinforcement ratio, F_u is the column peak load, ε_p is the strain correspondent to F_u, σ_c is the stress in concrete at F_u, σ_s is the longitudinal reinforcement stress at F_u, α is the inclination angle of the shear plane and, finally, IDpós is the column ductility index.

Table 2 - Variance analysis of the ε_p.

Variable	Sum of squares	Degrees of freedom	Mean squares	Mean square raio (F_o)	Minimum required for a factor to be significant ($F_{0.05,2,3}$)
Height	1,948957	2	0,974478	1286,16	9,55
Error	0,002273	3	0,000758	--	
Total	1,951230	5	--	--	

The column specimens were named of P-H-N, where H corresponds to the column height and N to the replicate number. Therefore, the specimen with the P 100-2 code means that it is the second specimen with 100 cm high. In Table 1 are presented the columns characteristics.

3.3 Instrumentation and test set-up

The specimens were tested on a rigid hydraulic press with load control, having a maximum load capacity of 2000 kN. The load was applied in a quasi-static mode with a load ratio of 35 kN/min. To ensure that the failure would occur in the instrumented region, the specimen ends were confined with a steel collar made from 12.5 mm steel plate with 10 cm large. They were fixed on the column's ends by four 19 mm diameter bolt with nuts made of high strength steel.

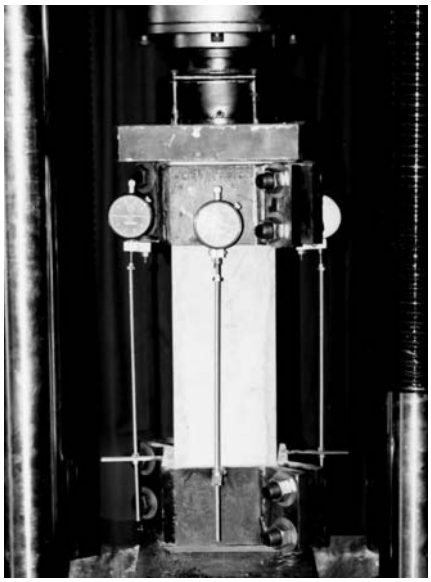

Figure 4 - Test set up.

Four dial gages were mounted, one on each column face, to measure the axial displacement. The dial gages were 0.01 mm precision and were attached to top and bottom steel collars clamped to the specimens to give a gage length of 279, 531 and 791 mm, to the columns with height of 50, 75 and 100 cm, respectively. The data readings were done at each load increment of 25 kN and the tests were stopped when the specimen strain reached 2.8%. In Figure 4, the details of the test set-up are showed.

4 Results and discussions

4.1 General behavior

The test procedure was able to get the entire post-peak behavior of the specimens. A uniform behavior was observed among the twin-specimens, in the maximum load, as well as in the ductility. The steel collars performed properly. Not only did they confine the columns ends, but also they assured the column to collapses in the tested region, not being observed cracks on the columns ends. It was not observed sliding between the specimens and the collar. The collapsed shear planes presented inclination between 42° and 49°, with average values and standard-deviation of 45.7° and 2.53°, respectively. Those values are consistent with the ones suggested by Hofbeck et al. [18] (45°). In Table 1, the value of the shear plane inclination angle of each column is presented.

The first set of cracks appeared on column faces close to the peak load and propagated vertically on the column's faces. The spalling of the concrete cover was observed in all specimens after the peak load had been reached. All specimens presented similar peak load, with average and standard deviation of 702 kN and 28.8 kN, respectively (Table 1). The buckling of the longitudinal reinforcement always happened subsequent to the peak load.

In Table 1, the strain correspondent to the peak load of each column is presented. The strains were calculated dividing the differential displacement by the gage length of each column. For the 50 cm high column, the mean peak strain was 4% and for the 100 cm high column this value was reduced to 2.65%. Apparently, it shows that the column gage length influences on the calculus of the plastic strain on the ascendant branch of the load vs. strain diagram. Aiming to confirm this observation, a variation analysis was performed. To perform the variance analysis, the significance of each factor effect was tested at confidence level of 95% using the F test [16]. In Table 2, the analysis results were presented. On the basis of the results, it is observed that the strain gage length influences on the strain calculus, on the ascendant branch of the column load vs. strain diagram at 95% confidence level. This fact shows that not only is strain gage length a factor that interferes on the descendant branch of load vs. strain diagram, but also that they influence the calculus of strains on the ascendant branch. Therefore, it is necessary to propose a methodology to calculate the strains to the descendant and to ascendant branch.

In Table 1, it is also presented the stress in the concrete and in the longitudinal reinforcement of the columns, when the peak load is reached. The stress in the longitudinal reinforcement were determined by the linear specific strain calculated by the ratio of the differential displacement read and the gage length and, considering, the steel mechanical properties presented before. To calculate the stress in the concrete the following procedures were adopted: the parcel of the ultimate column load supported by concrete was calculated subtracting the parcel of the load supported by the longitudinal reinforcement from the maximum column load; the ultimate compressive strength of concrete was

calculated dividing the ultimate load supported by the concrete cross area. It is observed that in the higher columns, the reinforcement did not reach the yield; nevertheless, this observation is masked by the usual procedure to calculate the strains. In addition, the mean concrete compressive strength was 34.47 MPa, with standard deviation of 1.68 MPa, whose values agree with the concrete compressive strengths gotten by cylinders specimens.

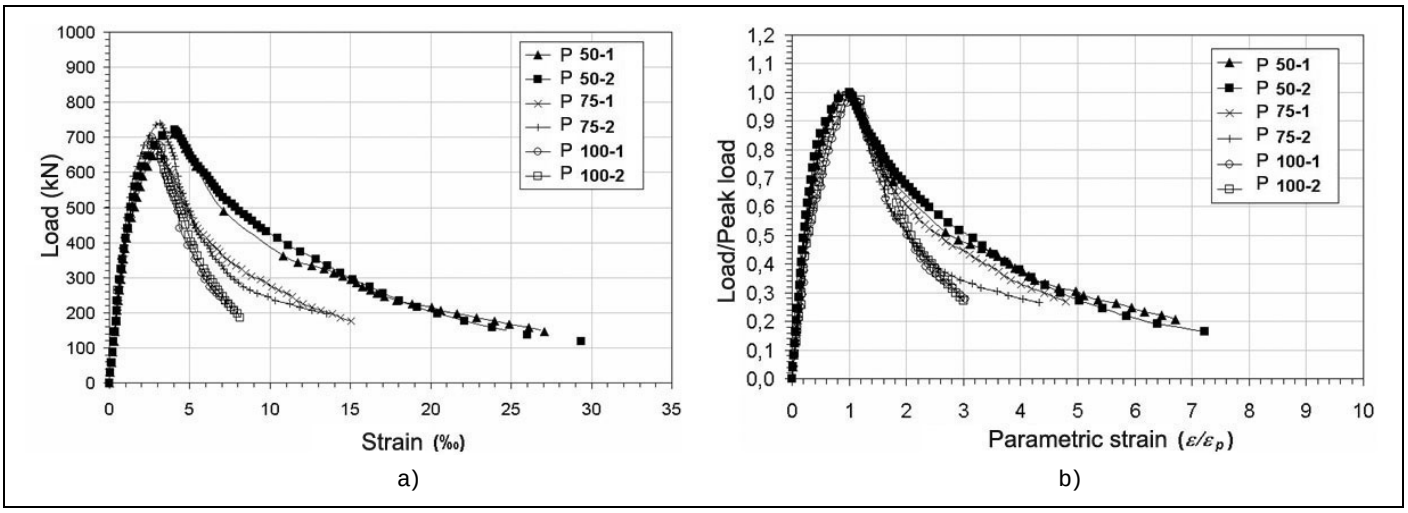

Figure 5 - Load vs. strain diagram: a) load vs. linear specific strain diagram and b) parametric load vs. parametric strain diagram.

Table 3 - Variance analysis of $ID_{pós}$ calculated using the usual procedure to strain quantification.

Variable	Sum of squares	Degrees of freedom	Mean squares	Mean square ratio (F_o)	Minimum required for a factor to be significant ($F_{0.05,2,3}$)
Height	0,123217	2	0,061609	18,77	9,55
Error	0,009846	3	0,003282	--	
Total	0,133063	5	--	--	

4.2 Ductility analysis

In Figure 5, the load vs. strain diagrams of tested columns are presented. To plot these diagrams, the linear specific strains were calculated dividing the average measured displacement by the gage length of each column. In Figure 5, the parametric load vs. strain diagram is also presented. It is evident that column with bigger gage lengths showed smaller strains at the descendant branch. In Table 1 is presented the ductility index calculated according to Eq.(1) and Eq.(2). The average values of the ductility index to the columns P50, P75 and P100 were 1.522, 1.343 and 1.171, respectively. To analyze the influence of the studied factor on the specimen ductility, a variation analysis was again performed, using the same procedure adopted before. The obtained results of the variance analysis are presented in Table 3. On the basis of those results, it is observed that the column height influence on the ductility index at confidence level of 95%. However, as the columns had the same physical and mechanical characteristics, they would have to present the same ductility index. Therefore, based on this analysis, it is attested that the use of the linear specific strain to represent the inelastic strain cause higher columns to present lower ductility index.

4.3 Proposed procedure to calculate the inelastic strain

The hypothesis that all column inelastic strain at the ascendant and descendant branch of the load vs. strain diagram stayed localized at the region that contains the shear plane was adopted. Moreover, according to Câmara et al. [5] observations, the extension of the shear plane can be calculated on basis of Eq.(3):

$$h_{aval} = b \cdot \tan(\alpha) \qquad (3)$$

where, b is the smallest dimension of the column cross section and α is the inclination angle of the shear plane, which can be assumed equal to 45° in the absence of experimental result. To calculate the ascendant branch of the load vs. strain diagram, it was adopted that all linear displacement follows the Hooke's Law. It was still adopted that after the linear part of the diagram, began the concrete plastification localized at the region of the shear plane. Therefore, the strains at the ascendant branch is defined by Eq.(4), Eq.(5) and Eq.(6):

$$\varepsilon_{elástica} = \frac{F}{K \cdot h_p} \quad (4)$$

$$\varepsilon_{plástica} = \frac{\delta - F/K}{h_{aval}} \quad (5)$$

$$\varepsilon_{pré-pico} = \varepsilon_{elástica} + \varepsilon_{plástica} \quad (6)$$

where, F is the applied load, h_p is the displacement gage length, K is the tangent elastic modulus of the column load vs. displacement diagram and δ is the differential measured displacement.

To calculate the strain at the descendant branch, it was adopted that all displacement increment resulting from the column plastification at the shear plane region and that the displacement proceeding from the strain softening at the column integral regions is transferred integrally to the shear plane. Thus, the strain at the ascendant branch can be given by Eq.(7):

$$\varepsilon_{pós-pico} = \varepsilon_p + \frac{\Delta\varepsilon_{elástica} \cdot \left(h_p - h_{aval}\right) + \Delta\delta}{h_{aval}} \quad (7)$$

where ε_p is the strain correspondent to the peak load, $\Delta\delta$ is the measured displacement increment after the peak load and $\Delta\varepsilon_{elastic}$ is the elastic strain decreasing in the column with the load reduction, which can be written by Eq.(8):

$$\Delta\varepsilon_{elástica} = \frac{F_u - F}{K \cdot \left(h_p - h_{aval}\right)} \quad (8)$$

Considering the proposed equations, the tested column strains were again calculated and the new load vs. strains diagrams are presented in Figure 6. At this time it is not evident which column is more ductile. The ductility indexes were again evaluated; nevertheless, the value of n suggested by Lima Jr. and Giongo [13] conducted to inaccuracy results. Therefore, it was taken equal to 5 and the results are presented in Table 4. A variation analysis was again performed, using the same procedure adopted before and considering confidence levels of 90% and 95%. In Table 5 the variance analysis results are presented and the gage length influence is not significant, even if a lower confidence level (90%) is considered. These results demonstrate that the proposed procedure to calculate the columns strain is not influenced by the strain gage length.

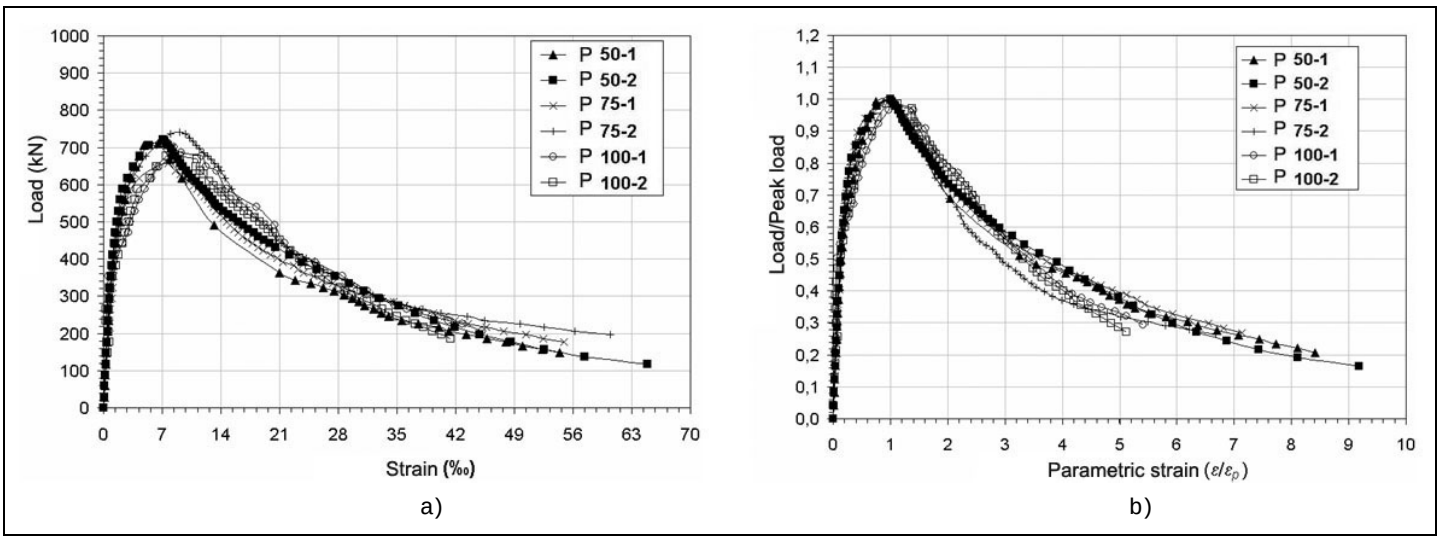

Figure 6 - Load vs. strain diagram carried out using the proposed procedure to strain quantification: a) load vs. linear specific strain diagram and b) parametric load vs. parametric strain diagram.

Table 4 - $ID_{pós}$ calculated using the proposed procedure to strain quantification.

Column					
P 50-1	P 50-2	P 75-1	P 75-2	P 100-1	P 100-2
2,583	2,757	2,681	2,655	2,490	2,595

Table 5 - Variance analysis of $ID_{pós}$ calculated using the proposed procedure to strain quantification.

Variable	Sum of squares	Degrees of freedom	Mean squares	Mean square ratio (F_o)	Minimum required for a factor to be significant ($F_{0.05,2,3}$) and ($F_{0.10,2,3}$)
Height	0,02134	2	0,01067	1,526	9,55 5,46
Error	0,02099	3	0,00699	--	
Total	0,04233	5	--	--	

5 Conclusions

1. The plastic strains at the ascendant and descendant branch of the load vs. strain diagram are influenced by the strain gage length, indicating that there is a plastic strain localization at the ascendant branch.
2. Higher columns presented smaller peak strain when the linear specific strain was considered.
3. The use of linear specific strain causes higher columns to present lower ductility indexes at a confidence of 95%.
4. A new procedure to calculate the column strain was proposed and its efficiency was attested by variance analysis.
5. Finally, the necessity of more experimental studies about the subject was evidenced.

6 Acknowledgements

The research was made possible through the support by grants of CNPq/MCT-Fundo Setorial de Infra-Estrutura and Fundação Araucaria and material donations of Camargo Correa Cimentos S.A and Telhavel. In addition, the tests were performed at the Laboratório de Tecnologia do Concreto da Hidrelétrica Itaipu/Binacional. The authors are grateful for the generous contributions.

7 Referências bibliográficas

[1] Cusson, D.; Larrard, F.; Boulay, C. e Pautre, P. Strain localization in confined high-strength concrete columns. J. Struc. Eng. ASCE. 122 (9), 1996, p.1055-1061.

[2] Mendes, H.O. Ductilidade de elementos de concreto de alta resistência. Dissertação de Mestrado - Universidade Federal do Rio de Janeiro/COOPE. Rio de Janeiro, 1993, 149.p.

[3] Aïticin, P.C. Concreto de alto desempenho. Editado por Pini Ltda, São Paulo, 2000, 667.p.

[4] FIB. Structural concrete - Textbook on behavior, design and performance. Updated knowledge of the CEB/FIP Model Code 1990. Comité Euro-International du Beton, v. 1, 1999, 224.p.

[5] Câmara, E.; Lima Júnior, H.C.; Willrich, F.L.; Fabro, G. e Giongo, J.S. Comportamento estrutural dos pilares dimensionados segundo o projeto de revisão da Norma NBR 6118 (2001). Revista Brasileira do Concreto - Instituto Brasileiro do Concreto, v.out/dez(31), 2002, p.46-61.

[6] Torrenti, J.M., Desrues, J., Benaija, E.H., e Boulay, C. Stereophotogrametry and localization in concrete under compression. J. Eng. Mech., ASCE 117(7), 1991, p.1455-1465.

[7] Van Mier, J.G.M. e Vonk, R.A. Fracture of concrete under multiaxial stress – recent developments. Material and Structures, 24, 1991, p.61-65.

[8] Van Vlack, L.H. Materials engineering. Edited by Addison Wesley Pub, 1982, 256.p.

[9] Ahmad, S.H. e Shah, S.P. Stress-strain curves of concrete confined by spiral reinforcement. ACI Journal, 79(6), 1982, p.484-490.

[10] Martinez, S.; Nilson, A.H. e Slate, F.C. Spirally reinforced high strength concrete columns. ACI Journal, 81(5), 1984, p.431-442.

[11] Cusson, D. e Pautre, P. Stress-strain model for confined high-strength concrete. J. Struc. Eng. ASCE. 121(3), 1995, p.468-477.

[12] Lima Jr., H.C. Avaliação da ductilidade de pilares de concreto armado, à flexo-compressão reta com e sem adição de fibras metálicas. Tese de Doutorado - Universidade de São Paulo, São Carlos, 2003, 322.p.

[13] Lima Júnior, H.C. e Giongo, J.S. Avaliação da ductilidade do concreto de alta resistência reforçado com fibras de aço. In: Anais do 43º Congresso Brasileiro do Concreto, Foz do Iguaçu, CD-ROOM I-025, 2001, p.1-16.

[14] ABNT. NBRNM248:2003 – Agregados: Determinação da composição granulométrica. Rio de Janeiro, 2003, 7.p.

[15] ABNT. NBRNM52:2003 – Agregado miúdo - Determinação de massa específica e massa específica aparente. Rio de Janeiro, 1987, 7.p.

[16] ABNT. NBRNM53:2003 – Agregado graúdo - Determinação de massa específica, massa específica aparente e absorção de água. Rio de Janeiro, 2003, 7.p.

[17] ABNT. NBR6118:2003 – Projeto de estruturas de concreto: Procedimentos. Rio de Janeiro, 2003, 232.p.

[18] Hofbeck, J.A.; Ibrahim, I.O. e Mattock, A.H. Shear transfer in reinforced concrete. ACI Journal, 66(2), 1969, p.119-128.

[19] Montgomery, D. . Design and analysis of experiments. Edited by John Wiley & sons. New York, 1984, 704.p.